RECENT ADVANCES IN WIDE-GAP DRIFT CHAMBERS DEVELOPING FOR THE SPECTROMETER HYPERON[1])

V. HLINKA, R. JANIK, P. POVINEC, B. SITÁR, Bratislava[2])
E. KLADIVA, B. SEMAN, J. ŠPALEK, Košice[3])
G. S. BITSADZE, Yu. A. BUDAGOV, V. V. GLAGOLEV, V. M. KOROLEV,
A. A. OMELYANENKO, A. A. SEMENOV, S. V. SERGEEV, Dubna[4])
A. M. BLIK, A. S. SOLOVYEV, Serpukhov[5])
A. B. YORDANOV, R. V. TSENOV, Sofia[6])
I. A. MINASHVILLI, Tbilisi[7])
A. M. ARTYKOV, Samarkand[8])
M. N. OMELYANENKO, Dubna[9])

Characteristics of wide-gap electrodeless drift chambers and their utilization for the measurement of electromagnetic shower position in the spectrometer HYPERON are described. The electrodeless drift chambers have several advantages: they can safely operate in high particle fiuxes ($>10^5$ particles s^{-1}), they have a small number of information channels, good spatial resolution and linearity, and a simple construction. Several methods of data processing from the wide-gap drift chambers are compared. The electrodeless drift chambers enable to reach a high efficiency and a very good spatial resolution of electromagnetic shower registration.

ПОСЛЕДНИЕ ДОСТИЖЕНИЯ В РАЗРАБОТКЕ ШИРОКОЗАЗОРНЫХ ДРЕЙФОВЫХ КАМЕР ДЛЯ СПЕКТРОМЕТРА «ГИПЕРОН»

В работе описываются характеристики широкозазорных безэлектродных дрейфовых камер и их применение для измерения координат электромагнитных ливней в спектрометре «ГИПЕРОН». Широкозазорные безэлектродные дрейфовые камеры обладают некоторыми преимуществами: они могут работать при больших потоках частиц ($>10^5$ частиц $с^{-1}$), используют малое количество информацион-

[1]) Dedicated to the 30th anniversary of the foundation of the Joint Institute for Nuclear Research, Dubna.

[2]) Comenius University, 842 15 BRATISLAVA, Czechoslovakia.
[3]) Institute of Experimental Physics, Slov. Acad. Sci., KOŠICE, Czechoslovakia.
4) Joint Inst. for Nuclear Research, DUBNA, USSR.
[5]) Inst. of High Energy Physics. SERPUKHOV, USSR.
[6]) University of Sofia, SOFIA, Bulgaria.
[7]) University of Tbilisi, TBILISI, USSR.
[8]) University of Samarkand, SAMARKAND, USSR
[9]) MIREA, DUBNA, USSR.

ных каналов, имеют хорошее пространственное разрешение, линейность и простую конструкцию. Сравниваются различные методы обработки сигналов из широкозазорных дрейфовых камер. Безэлектродные дрейфовые камеры позволяют достигать высокую эффективность и очень хорошее пространственное разрешение в определении координат электромагнитных ливней.

I. INTRODUCTION

Particle detectors in high energy physics experiments have enormous dimensions and a large number of electronic channels ($\sim 10^5$) is necessary for signal processing. Therefore, it is important to search for new ways how to make large, but less complicated and less expensive detectors.

For coordinate detectors this means to use drift chambers instead of more expensive and less precise proportional chambers. Drift chambers with gaps of 20 – 25 mm are mostly used. However, in areas far from the beam zone, chambers with large drift gaps (50—100 mm) could be used without significant losses in the accuracy of particle localization. These, the so-called wide-gap drift chambers can be about 10 times less expensive than the common drift chambers or proportional chambers.

In the present paper we discuss characteristics of electrodeless drift chambers and their utilization for the measurement of the electromagnetic shower position in the high energy spectrometer HYPERON.

II. ELECTRODELESS DRIFT CHAMBERS

Recently a new type of wide-gap chambers — electrodeless drift chambers — has been proposed [1, 2]. There are no field-shaping electrodes in them and the necessary homogeneous electric field is created by a positive ion deposition on the chamber walls made from an insulator [1—4].

There is no doubt about the advantages of the electrodeless drift chambers, e. g. a drift of electrons over a distance of about 1 m can be performed in such a chamber.

The electrodeless drift chambers have been used only in low-intensity particle fluxes from radioactive sources or cosmic radiation. It has been pointed out [4] that these chambers cannot be used in higher-intensity particle beams, because a large positive charge is accumulated on the insulator surface, which leads to loss of the efficiency in the chamber. Having analysed processes in the electrodeless drift chamber, we realized that a proper choice of material for the chamber construction and a higher sensitivity of electronics should allow to use the chamber in high intensity particle beams. In our previous work [5] we tested for the first time the characteristics of the electrodeless drift chamber in a flux of more than 10^5 particles s^{-1} per wire. In this paper we present the results of new measurements.

Fig. 1 shows a diagram of wide-gap drift chambers. The electrode chamber (Fig. 1a) is shown for comparison with the electrodeless drift chambers (Fig. 1b, 1c and 1d). The principle of the field shaping by positive ions deposited on the insulating walls of the chamber is shown in Fig. 1b. In the chambers with gain-control electrodes (100 μm thick wires stretched near the fibre-glass surface parallel to the signal wire, Fig. 1 c, d) the field is also shaped mainly by positive ion deposition. All chambers had walls made of fibre-glass 1.5 mm thick (mark SF [5]) with earthed copper foils on their outer side. All chambers were 20 mm thick with a maximum drift length of 100 mm. Signal wires of 30 μm in diameter were used. The dimensions of the chambers (a) and (b) were $200 \times 300 \times 200$ mm^3 with 1 signal wire, chambers (c) and (d) were $1000 \times 1000 \times 2000$ mm^3 with 5 signal wires (Fig. 1d for simplicity shows only one signal wire). A gas mixture of 82 % argon and 18 % isobutane was used as the gas filling of the drift chambers.

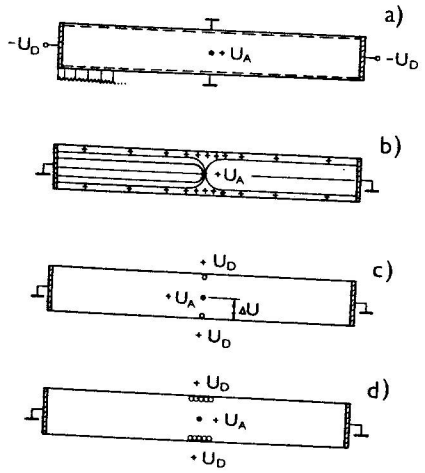

Fig. 1. Electrode (a) and electrodeless drift chambers (b, c, d). U_A — the anode voltage, U_d — the voltage on the field shaping electrodes.

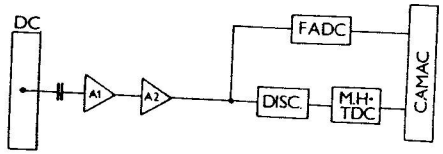

Fig. 2. The block scheme of the electronics. DC — drift chamber, A1, A2 — amplifiers, DISC — discriminator, F ADC — flash ADC, M. H. TDC — multi hit TDC.

The chambers were tested in e^+, π^+ and proton beams with the energy of 3—12 GeV on the IHEP accelerator at Serpukhov. The block diagram of the electronics used in the experiments is shown in Fig. 2. The amplifier A1 has a gain 0.6 V/μA, the amplifier A2 has a regulating gain from 1 to 10. A detailed description of the used multi-hit TDC and flash ADC is published elsewhere [6, 7].

Using the chamber shown in Fig. 1b we measured the mean amplitude of the signal and the mean charge, sampled in drift chamber over many hundred volts. Their dependence upon the voltage on the signal wire U_A is shown in Fig. 3. The couting characteristic of this chamber is shown in Fig. 4. A typical long plateau (~ 2 kV) has been obtained.

In the electrodeless drift chamber it is practically impossible to change the signal amplitude by changing the anode voltage. One way how to change the amplitude of the signal is to introduce the gas gain-control electrodes. We noticed that one wire on each side of the sense wire (Fig. 1c) does not change effectively the gas gain. This should be done using two strips on the wall surface, or using more wires to form a strip (2 mm wide in our case, see Fig. 1d).

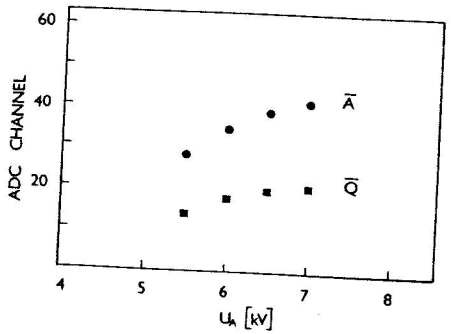

Fig. 3. The mean amplitude ($\bar{A}$) and the mean charge ($\bar{Q}$) as functions of the anode voltage in the electrodeless drift chamber.

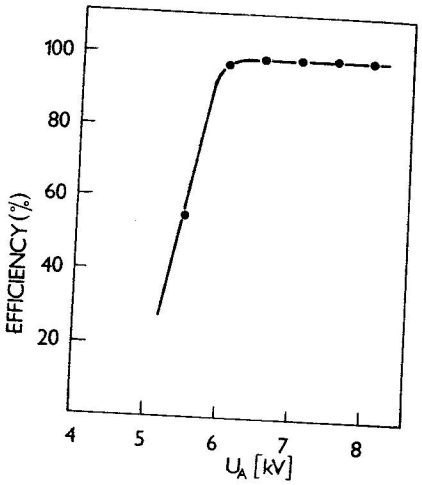

Fig. 4. The efficiency of the electrodeless drift chamber vs the anode voltage.

The other way how to change the amplitude of the signal is to use an additional aplifier. Our amplifier (A2 in Fig. 2) can change the amplitude ten times, that is enough for obtaining a high efficiency. The chaber (1d) is efficient over the whole sensitive volume, as shown in Fig. 5. In this figure also the track efficiency is shown, obtained after reconstruction of tracks in three drift chambers. There is a good linearity between the measured drift time and the particle coordinate, shown in Fig. 6. From this dependence necessary constants — the drift velocity and the overall delays are found. It can be seen that the drift velocity in similar chambers ((1), (2)) is equal.

A good spatial resolution was achieved in the large electrodeless drift chamber (type 1d). The resolution changes as $\sqrt{x}$ from 250 μm at $x = 10$ mm to 400 μm at $x = 100$ mm (Fig. 7), where x is the drift distance.

The electrodeless drift chambers could work in relatively high particle fluxes

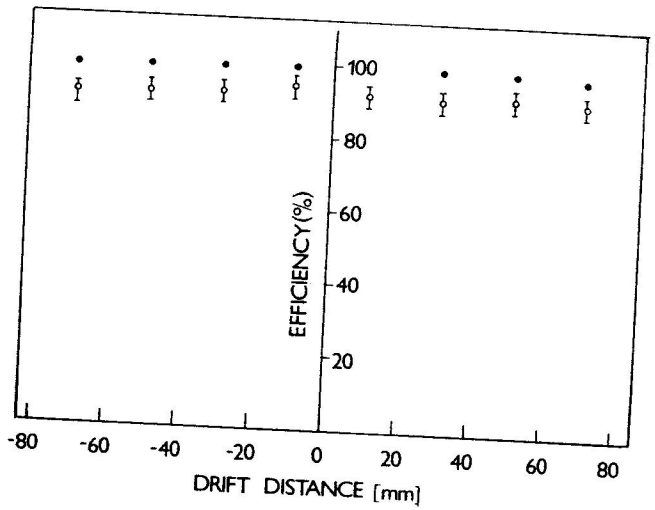

Fig. 5. The full efficiency (●) and the track efficiency (○) as a function of the drift distance.

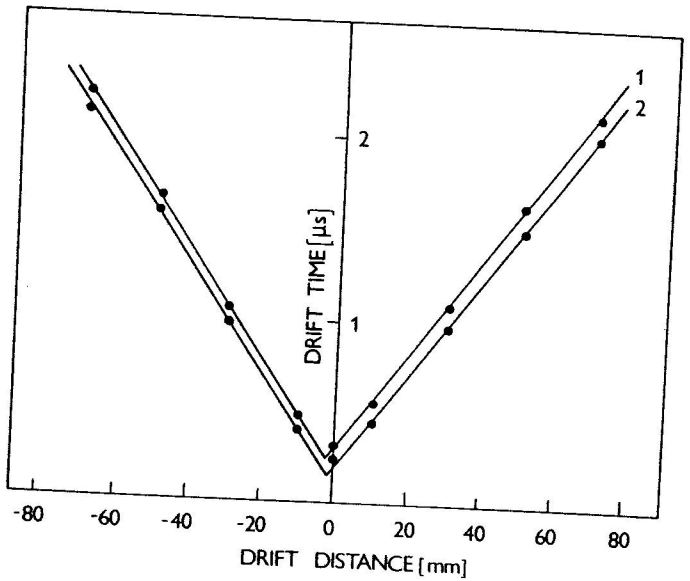

Fig. 6. The measured drift time vs the particle coordinate (drift distance) in two electrodeless drift chambers.

($>10^5$ particles s^{-1} per wire). A drop in the amplitude caused by the space charge accumulation can be compensated in the case of high flux rates by an amplification (in the amplifier A2). In Fig. 8 the efficiency of the chamber (type 1d) as a function of the flux rate for two different amplification values is shown. In the case of a higher amplification (A_2) we did not see the change of efficiency with the flux rate. neither did other parameters, e. g. the measured coordinate, of the spatial resolution change with the flux rate [5].

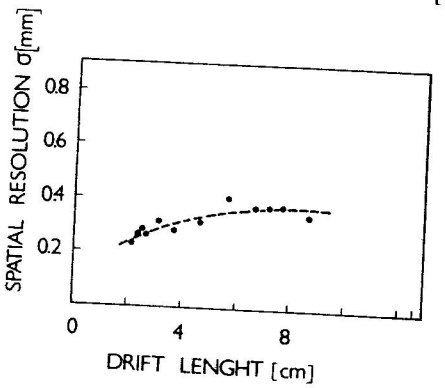

Fig. 7. The spatial resolution vs the drift length X. The line corresponds to function $\sqrt{X}$.

We built four chambers 1×1 m^2 with 5 sense wires each (type 1d). The chambers are very compact and light with frames only 30 mm wide. The full thickness of the chamber (including frames and electronics) is 25 mm, their weight is ~ 5 kg.

III. MEASUREMENT OF ELECTROMAGNETIC SHOWER POSITION WITH WIDE-GAP DRIFT CHAMBERS

The wide-gap drift chambers have been successfully applied for measurement of coordinates of electromagnetic showers in the spectrometer HYPERON.

Experiments have been carried out at channel no. 18 at IHEP-Serpukhov in the 3 GeV positron beam. A layout of the experiment is shown in Fig. 9. The trigger consists of 3 scintillation counters S_1, S_2 and S_3, Cherenkov counters C_1, C_2 and C_3 and narrow scintillation counters S_4 and S_5 (1 mm width). The shower energy was determined by the Cherenkov shower lead-glass detectors consisting of 12 lead-glass TF-1-000 counters with dimensions $100 \times 1000 \times 350$ mm^3 each. In front of the lead detector there is an active converter made of the same lead-glass (the rediation length $X_0 = 25$ mm). For further analysis we selected those events where the measured shower energy coincided with the beam energy within the energy resolution of the detector ($\Delta E/E \sim 6$ %). The impact point of a particle at the converter was determined by the drift chamber DC-1. This is the electrode

wide-gap chamber (type 1 a) of $200 \times 300 \times 20$ mm^3 with one anode and the drift length of 100 mm. The chamber had on the inner surface copper strips parallel to the wire 1.5 mm wide with a 5 mm pitch. At the distance of 100 mm from the signal wire there are electrodes under voltage $-U_D$. A divider with an accuracy of ≤ 0.5 % was used to produce a linear potential on the strips. The coordinate of the shower axis was determined by the drift chamber DC-2 placed 10 mm behind the converter (the electrodeless wide-gap chamber, type 1b, of $200 \times 300 \times 20$ mm^3 with one anode and the drift length of 100 mm). A gas mixture of 82 % argon and 18 % isobutane was used as the gas filling of the drift chambers. The block scheme of the electronics is shown in Fig. 2.

To determine the coordinate of the shower axis the position of maximum charge density, corresponding to the centre of the high energy conversion electron jet, was measured. The axis of such a jet follows in principle the direction of the gamma-quantum (electron) entering the converter. To fix the position of the maximum charge density, the charge from adjacent electron and positron tracks is integrated both inside the drift chamber and in the electronics. As a result the strongest signal corresponds to the central jet of the shower, while small amplitude signals correspond to single electrons far from the shower axis. Choosing the optimum threshold one may reject most of the small signals from single electrons, maintaining at the same time a high efficiency of shower detection.

The electron drift time from the shower axis depends linearly on the coordinate. The drift velocity found from these measurements is about 5 cm/μs at a field strangth of about 600 V/cm and it does not depend on the voltage in the interval 500—700 V/cm.

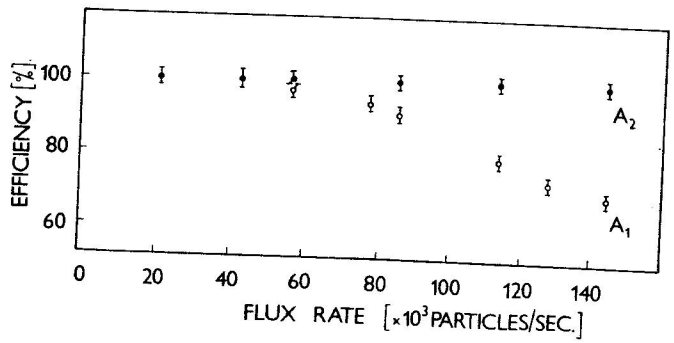

Fig. 8. The efficiency of the electrodeless drift chamber vs the flux rate per wire for two amplification coefficients A_1 and A_2 ($A_2 > A_1$).

Two methods have been used for the shower-position determination, based on the flash ADC [7] and the multi hit TDC [8]. In the ADC method the signal is quantized in ADC and stored in the buffer memory every 64 ns. Fig. 10 shows

a typical histogram of the charge distribution from a shower registered by the chamber DC-2. In the second method the signal goes through the zero crossing discriminator and the multi hit time to digital converter with a small dead time (64 ns) that quantizes the position of the maxima of signals with an accuracy of about 1 ns ($\sim 50\ \mu$m in space).

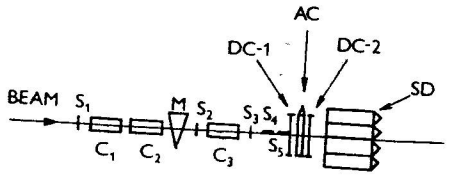

Fig. 9. The experimental set-up. S_1, S_2, S_3, S_4 and S_5 – scintillation counters, C_1, C_2 and C_3 — Cherenkov counters, DC-1 and DC-2 — drift chambers, AC — active lead glass converter, SD — shower lead glass detector, M — magnet.

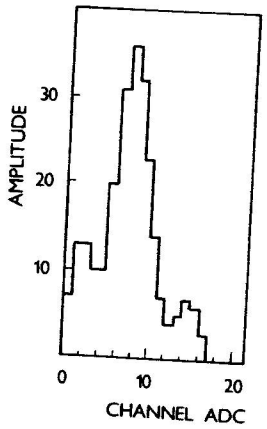

Fig. 10. The spectrum of the charge distribution from a shower registered by the drift chamber as obtained at the output of ADC.

The coordinate resolution for showers is determined from the distribution of the values $\Delta X = X_1 - X_2$, where X_1 is the impact point for the high-energy positron at the converter, determined by the DC-1; and X_2 is the shower axis coordinate, determined in the DC-2.

Methods of determination of the coordinate X_2 were discussed in [9]. Here we shall compare results obtained by 4 methods:

i) the TDC method

ii) the ADC method — centre of gravity; here the shower coordinate of the centre of gravity of the ADC spectrum

$$X_2 = \sum_i A_i X_i \Big/ \sum_i A_i,$$

where A_i represents the height of the signal in the i-channel of ADC ($i = 1, 2, \ldots, 256$) and X_i is the coordinate determining the position A_i

III) the ADC method — maximum; here the shower coordinate was approximated by the channel of ADC with the maximum value of A_i

iv) the ADC method — weighted maximum; here the shower coordinate was

obtained by weighting one part of the signal with maximum amplitude. This part consisted of the channel with maximum amplitude and two channels from the right and left side.

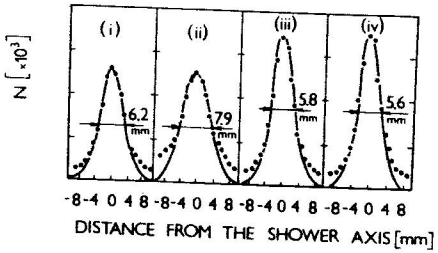

Fig. 11. The distribution $\Delta X = X_1 - X_2$ as obtained by various methods. The thickness of the converter was $4X_0$.

The space resolution of the chamber was obtained from the distribution $\Delta X = X_1 - X_2$. Fig. 11 compares these distributions as obtained by the above discussed methods. All distributions were measured simultaneously under the same experimental conditions. The thickness of the converter in these measurements was $4X_0$. The measured distributions were fitted by gaussians. Although the calculated distributions do not fit experimental points at larger distances from the shower axis, this approximation is used as it enables us to compare FWHM obtained in various experiments published in literature.

The resolution σ_{sh} defined as $\sigma_{sh} = \text{FWHM}/2.35$ obtained over the full surface of the drift chamber, except the points close to the wire (−5, 15 mm), for the converter thickness of $3X_0$ is listed in Tab. 1. The presented values were not corrected for the beam divergence and for the own resolution of drift chambers ($\sigma \sim 0.3$ mm). It can be seen from Tab. 1 that, except for the method "ADC — centre of gravity", the spatial resolution obtained by other methods is similar.

Furthermore we studied possible distortions in the determination of the shower coordinate due to accumulation of the space charge in the electrodeless drift chamber when the beam flux is large. As follows from Fig. 12a, distortions are not observed. The space resolution does not depend on the flux, Fig. 12b.

Table 1
Comparison of methods of data processing

Method	Resolution σ_{sh} [mm]
ADC — weighted maximum	1.9 ± 0.1
ADC — maximum	2.0 ± 0.1
TDC	2.1 ± 0.1
ADC — centre of gravity	2.6 ± 0.1

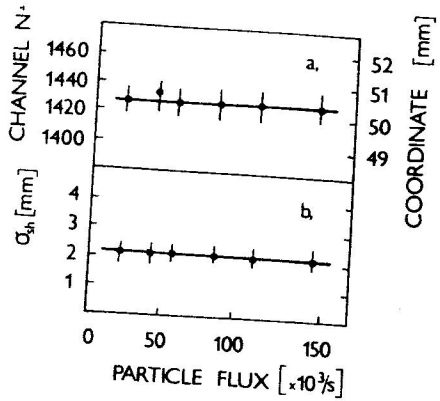

Fig. 12. The measured coordinate (a) and the spatial resolution for showers (b) vs the flux. The coordinate of showers was measured with the TDC method.

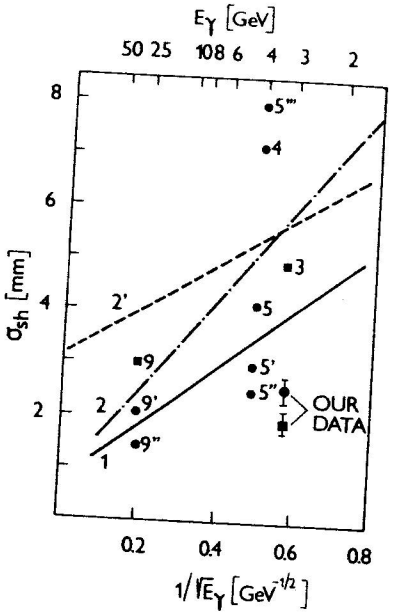

Fig. 13. The spatial resolution for showers measured in calorimeters with one converter and one coordinate detector vs the energy (for explanation see the text).

The best results of the spatial resolution for electromagnetic showers, obtained in different experiments and by different methods are compared in Fig. 13. Only devices with one converter and one coordinate detector, not multilayer calorimeters, are presented. In [10, 11] the dependence of the resolution on the incident electron (gamma-quantum) energy E_γ was measured by means of scintillation hodoscopes and self-quenching streamer tubes (lines 1, 2 and 2′ in Fig. 13). The simplest method to obtain the shower axis coordinate is to calculate the centre of gravity of the ionisation charge. CERN [12] and Serpukhov groups [13] calculated beside calculations of centre of gravity (points 5 and 9) also the coordinate taking into account the exponential drop of the charge across the shower, which improves the resolution (point 9′). Fitting by the calculated function further improves the resolution (points 5′, 5″ and 9″). The worst resolution was obtained using the proportional chamber without ADC (point 5‴). The resolution was improved [12] when instead of reading from the anodes of the proportional chamber (point 5′) an induced charge from the cathodes was used for shower

position determination (point 5″). Our data in Fig. 13 (lowest point is corrected for the beam divergence) for the given energy show the best spatial resolution of electromagnetic shower registration.

IV. CONCLUSIONS

The wide-gap electrode and electrodeless drift chambers have proved to be very useful devices in high energy physics experiments. We have found that especially the electrodeless drift chambers have several advantages. They can safely operate in high particle fluxes, they have a small number of information channels, good spatial resolution and linearity, and a simple construction.

The measurement of the electromagnetic shower position with the electrodeless drift chamber has shown the excellent characteristics of this detector. Several methods of data processing from these chambers were compared. It has been found that the best spatial resolution was obtained using the ADC method of weighted maximum, the ADC method of maximum and the TDC method. The electrodeless drift chambers have enabled to reach a high efficiency and a very good spatial resolution of electromagnetic shower registration at relatively high fluxes.

The authors are indebted to V. P. Dzhelepov, V. B. Flyagin and M. V. Kutin for supporting our work and to other members of the Hyperon collaboration for assistance in the test beam experiments.

REFERENCES

[1] Allison, J. et al.: Nucl. Instr. and Meth. *201* (1982), 341.
[2] Becker, Ch., Weihs, W., Zech, G.: Nucl. Instr. and Meth. *200* (1982), 335.
[3] Zech, G.: Nucl. Instr. and Meth. *217* (1983), 209.
[4] Becker, Ch., Weiks, W., Zech, G.: Nucl. Inst. and Meth. *213* (1983), 243.
[5] Budagov, Yu. A. et al.: Nucl. Instr. and Meth. A *238* (1985), 245.
[6] Budagov, Yu. A. et al.: Nucl. Instr. and Meth. A *234* (1985), 302.
[7] Budagov, Yu. A. et al.: Preprint JINR 13-85-585, Dubna 1985.
[8] Budagov, Yu. A. et al.: Preprint JINR 13-84-757, Dubna 1984.
[9] Bicadze, G. S. et al.: Preprint JINR 13-85-694, Dubna 1985.
[10] Cox, B. et al.: Nucl. Instr. and Meth. *219* (1984), 491.
[11] Rameika, R. et al.: IEEE Trans. Nucl. Sci. NS-*31* (1984), 60.
[12] Gabathuler, E. et al.: Nucl. Instr. and Meth. *157* (1978), 47.
[13] Akopdjanov, G. A. et al.: Nucl. Instr. and Meth. *140* (1977), 441.

Received December 16th, 1985
Revised version received January 21, 1986